Advances in Geo-Energy Research

Vol. 6, No. 6, p. 460-471, 2022

Original article

Effect of viscosity and heterogeneity on dispersion in porous media during miscible flooding processes

Zhenqiang Bai[1,2], Kaoping Song[1,3]*, Hongtao Fu[3], Yu Shi[4], Yang Liu[5], Zhuo Chen[6]

[1]*School of Petroleum Engineering, Northeast Petroleum University, Daqing, 163318, P. R. China*

[2]*Research Institute of Exploration and Development of Daqing Oilfield Company Ltd., Daqing, 163453, P. R. China*

[3]*Unconventional Petroleum Research Institute, China University of Petroleum (Beijing), Beijing 102249, P. R. China*

[4]*School of Petroleum Engineering, Xi'an Shiyou University, Xi'an 710065, P. R. China*

[5]*Oil Production Plant No.1 of Changqing Oilfield Company, Yanan 716000, P. R. China*

[6]*School of Mining and Petroleum Engineering, University of Alberta, Edmonton T6G 2R3, Canada*

Keywords:
Pore scale
heterogeneity
dispersion
miscible flooding

Cited as:
Bai, Z., Song, K., Fu, H., Shi, Y., Liu, Y., Chen, Z. Effect of viscosity and heterogeneity on dispersion in porous media during miscible flooding processes. Advances in Geo-Energy Research, 2022, 6(6): 460-471.
https://doi.org/10.46690/ager.2022.06.03

Abstract:
In this paper, a mathematical model has been developed to quantitatively examine the effect of viscosity and heterogeneity on dispersion in porous media at the pore scale during miscible flooding processes. More specifically, the Navier-Stokes equation and advection-diffusion equation are coupled with supplementary equations to describe the solvent transport behaviour. Two-dimensional heterogeneous models are numerically developed as a function of porosity and permeability, assuming that the grain sizes satisfy normal distribution. In addition, the performance of miscible hydrocarbon gas injection in heterogeneous porous media is comprehensively evaluated. It is found that a larger aspect ratio (ratio of pore throat size) in the single non-flowing pore model results in a greater asymmetry of the concentration curve. As for single non-flowing pore models and heterogeneous models, the dispersion coefficients increase with the expansion of the non-flowing domain. Both the heterogeneity of porous media and the variable viscosity of the fluid mixture contribute to the asymmetry of the concentration curve in the heterogeneous model. A negative correlation is established between the sorting coefficients of pore throat size and the power-law coefficients. As for slug injection, the injected solvent slug size along the longitudinal direction does not effectively influence the longitudinal length of the mixing zone for a given porous medium and fluids, though the Peclet number and the porosity greatly affect the length and concentration distribution of the mixing zone.

1. Introduction

Miscible gas flooding has proved to be an effective technique for enhancing oil recovery (Arshad et al., 2009; Brodie et al., 2012). During miscible gas flooding processes, for a given concentration of the injected gas or solvent, its distribution in porous media will be significantly affected by the fluid flow. In most hydrocarbon reservoirs, the presence of heterogeneity always generates statistically complex morphologies, resulting in complicated flow behaviours (Berkowitz and Scher, 2001). On the other hand, the heterogeneous distribution of a miscible fluid in porous media further aggravates its flow complexity (Dullien, 1992; Golparvar et al., 2018; Panja et al., 2020). Therefore, it is of fundamental practical importance to quantify the flow behaviour of gas/solvent transport in porous media under miscible conditions, so that the reservoir fluids flow performance can be accurately evaluated.

Since the 1980s, numerous efforts have been made to experimentally and theoretically determine the relationship between dispersion and the properties of porous media in the laboratory (Bretz et al., 1988; Delgado, 2007). At the early stage, experiments found that the relationship between the ratio of longitudinal dispersion coefficient to the diffusion

Yandy Scientific Press

*Corresponding author.
E-mail address: baizhenqiang@petrochina.com.cn (Z. Bai); songkaoping@cup.edu.cn (K. Song); fuhongtao02@163.com (H. Fu); liuyang029@126.com (Y. Liu); shiyuywy@126.com (Y. Shi); zhuo8@ualberta.ca (Z. Chen).

Received April 20, 2022; revised May 19, 2022; accepted May 28, 2022; available online June 6, 2022.

coefficient and the Peclet number is a function of particle size. The effluent solute concentration shows dependence on the heterogeneity of porous media at the pore scale (Bretz and Orr, 1987; Fourar et al., 2005). The injected fluid may cause early breakthrough because of the heterogeneity of porous media, leaving a long tail on the effluent solute concentration curve (Bretz et al., 1986). Theoretically, the solute concentration in a single capillary tube can be analytically obtained using proper boundary conditions once the orientation of fluid flow has been determined. As for porous media (both unconsolidated sandpacks and consolidated rocks), the flow channels are usually considered as a network with random size and flow conductivity. The performance of fluid flow in such network has been described as the summation of random and complicated phenomena caused by the randomness of network in the porous media. Furthermore, a mathematical model was proposed to characterize the asymmetric solute concentration by dividing the pore space of porous media into flowing and non-flowing fractions. Subsequently, a similar porous-sphere model and transverse-matrix-diffusion model were proposed for such a characterization purpose by Correa et al. (1990).

In the 21st century, probabilistic approaches were introduced to quantitatively represent the characteristics of non-Fickian transport in porous media (Berkowitz and Scher, 2001; Berkowitz et al., 2006). Based on the Lagrangian-based random-walk network model, Bijeljic et al. (2004) calculated the power-law coefficients of correlation between D_L/D_O (the ratio of longitudinal dispersion coefficient (D_L) to diffusion coefficient (D_O)) and the Peclet number for the reconstructed Berea samples. The calculated power-law coefficient was equal to 1.24, which is in good agreement with the experimental measurements for sandstones. Also, the advection-diffusion equation associated with the network of flow channels of porous media has been numerically developed to quantify the non-Fickian transport behaviour (Cao and Kitanidis, 1998; Garmeh et al., 2009; Jha et al., 2009). Accordingly, Garmeh et al. (2009) obtained the power-law coefficients in the range of 1.55 to 1.89 by simulating the performance of homogeneous unconsolidated porous media, which were higher than those of well-packed porous media. Although there have been great improvements in understanding the non-Fickian dispersion at the pore scale by directly obtaining the solute concentration distribution in porous media, no attempts have been made to quantify the relationship among pore structure, velocity field and solute transport because of the extremely complex flow behaviour (Bijeljic et al., 2013).

Recently, with the progress of computer technology, scholars in P. R. China and abroad have carried out a lot of research on the influence of different injected fluids and the heterogeneity of porous media on dispersion. Muhammad et al. (2019) found that the dispersion coefficient increased with a decrease in permeability, with Bandera Grey having the highest dispersion coefficient and invariably higher mixing between the injected CO_2 and the nascent CH_4. Peyman et al. (2018) proposed a robust numerical workflow for the simulation of miscible-floods in unsaturated porous media and investigated the impact of matrix heterogeneity, connate water, cementation, and injection velocity on the longitudinal dispersion coefficient. Dispersion and the mixing of fluids during miscible displacement in porous media are known to be strongly affected by heterogeneity and viscous fingering. In Afshari's study, direct pore-level numerical simulations were employed to model flow and solute transport during both stable and unstable miscible displacements in two-dimensional packings of circular grains (Saied et al., 2018). Mahnaz et al. (2016) studied the effect of pore-scale heterogeneity, in particular the pore-size distribution and pore connectivity as well as mobility ratio M on miscible displacements, and obtained the effective longitudinal dispersion coefficient as a function of M. Concerning the importance of accounting for the micro-scale correlation lengths in predictive stochastic pore-scale modeling, the estimated dispersion coefficients were found to increase in correlated networks compared to uncorrelated ones in the advection-controlled regime (Majdalani et al., 2015; Babaei and Joekar-Niasar, 2016; Sheng et al., 2020; Yang et al., 2020). In general, the dispersion of different types of porous media can be determined at the pore scale, however, the effects of fluid properties have not been taken into account.

In this paper, a mathematical model has been formulated to quantitatively examine the effects of properties of both porous media and fluids on dispersion at the pore scale during miscible flooding processes. The classical Navier-Stokes equation is employed to obtain the deterministic flow velocity field in the flow channels of porous media. This flow velocity field makes it possible to calculate the concentration distribution of entire porous media using the advection-diffusion equation. The effect of viscosity and heterogeneity on dispersion in porous media during miscible flooding processes is quantitatively analyzed on the basis of the dispersion of different types of porous media. First, a supplementary equation is applied with respect to the fluids mixture property to quantitatively describe the viscosity as a function of solvent concentration. The dispersion processes can then be quantified by simultaneously solving the aforementioned equation matrix. Randomly distributed circle grains are employed to numerically form a heterogeneous porous medium model, assuming that their sizes follow normal distribution. The variable permeability and porosity of such models are obtained by varying the mean and variance of grain sizes. The miscible flooding processes of continuous/slug injections in heterogeneous porous models are subsequently simulated over a range of flow conditions. Then, the effects of various parameters associated with pore structure on dispersion processes are extensively analyzed and discussed.

2. Mathematical formulation

2.1 Navier-stokes equation and continuum equation

In practice, porous media can be treated as a network of flow channels, in which the flow behaviour can be described by using the Navier-Stokes equation (Yang et al., 2013). The classic Navier-Stokes equation for incompressible Newtonian fluid is expressed as follows:

$$\frac{\partial V}{\partial t} + V \cdot \nabla V = -\frac{1}{\rho}\nabla P + \mu \nabla^2 V + f \tag{1}$$

As for the mass continuity equation:

$$\nabla V = 0 \tag{2}$$

By combining Eqs. (1) and (2), the unsteady-state Navier-Stokes equation with variable viscosity can be expressed as follows:

$$\rho\left(\frac{\partial V}{\partial t} + V\cdot\nabla V\right) = -\nabla P + \nabla(\mu\cdot\nabla V) \tag{3}$$

where V denotes velocity vector, m/s; ρ denotes the density of fluids mixture, g/cm^3; t denotes time, s; P denotes pressure, Pa; μ denotes the viscosity of fluids mixture, Pa·s; f is 0 (horizontal small-scale simulation), and gravity is ignored.

The following six dimensionless variables and one dimensionless parameter are introduced and utilized to nondimensionalize the aforementioned equations:

$$\begin{cases} x_D = \dfrac{x}{L_c} \\ y_D = \dfrac{y}{L_c} \\ P_D = \dfrac{P}{\rho v_i^2} \\ R_e = \dfrac{\rho v_i L_c}{\mu} \\ t_D = \dfrac{v_t t}{L_c} \\ V_{D_x} = \dfrac{v_x}{v_i} \\ V_{Dy} = \dfrac{v_y}{v_i} \end{cases} \tag{4}$$

where L_c denotes characteristic length, m; v_i denotes average interstitial velocity in porous media, m/s; x_D and y_D are respectively dimensionless length in the x and y direction; P_D denotes dimensionless pressure; t_D denotes dimensionless time; V_{Dx} and V_{Dy} respectively denote dimensionless velocity in the x and y directions; x and y denote the length of x, y direction, m; R_e denotes Reynolds number; v_t denotes velocity at time t, s; and v_x and v_y respectively denote velocity in the x and y directions, m/s. The dimensionless Eqs. (2) and (3) can be expressed as:

$$\nabla V_D = 0 \tag{5}$$

$$\frac{\partial V_D}{\partial t_D} + (V_D\cdot\nabla V_D) = -\nabla P_D + \nabla\left(\frac{1}{Re}\cdot\nabla V_D\right) \tag{6}$$

2.2 Advection-diffusion equation

In general, the dispersion process includes three mechanisms in porous media, i.e., (1) molecular diffusion; (2) advective motion with the mean velocity field of the flow; and (3) hydrodynamic dispersion of the solute (Ghazanfari et al., 2010). Based on Fick's law, the advection-diffusion equation can be obtained as follows:

$$\frac{\partial c}{\partial t} = D_o\nabla^2 c - V\nabla c \tag{7}$$

where c denotes concentration, mg/L; D_o is diffusion coefficient.

Similarly, two-parameter groups are introduced into Eq. (7), which can be written as:

$$\frac{\partial c_D}{\partial t_D} = \frac{1}{P_e}\nabla^2 c_D - V_D\nabla c_D \tag{8}$$

$$\begin{cases} c_D = \dfrac{c - c_{ini}}{c_{inlet} - c_{ini}} \\ Pe = \dfrac{v_i L_c}{D_o} \end{cases} \tag{9}$$

where c_D denotes dimensionless concentration; c_{inlet} denotes injection concentration at the inlet, mg/L; c_{ini} denotes the initial concentration of solvent in porous media, mg/L; and Pe is Peclet number.

2.3 Supplementary equation

The injected gas/solvent usually imposes a strong impact on the viscosity of displaced fluids (Turta et al., 1999; Wen and Kantzas, 2004; Booth, 2008). Based on Eqs. (6) and (8), viscosity affects flow velocity and in turn the solvent concentration distribution in porous media. The viscosity of the mixture between solvent and oil was found to be mainly affected by the solvent concentration under constant temperature and pressure (Turta et al., 1999; Srivastava et al., 2000). Thus, solvent concentration can also reversely change the viscosity of mixture during miscible flooding. To couple the Navier-Stokes equation with the advection-diffusion equation, the flow behaviour of a solvent transport in porous media can be described if a supplementary equation is introduced in terms of the PVT properties of a reservoir fluid-solvent mixture.

Hydrocarbon, such as methane, propane and butane, can achieve first contact miscibility with crude oil under certain conditions (Sahimi et al., 2006). In this study, it is assumed that first contact miscible flooding can be reached once the hydrocarbon gas gets into contact with crude oil. This assumption is to ensure that there is single-phase fluid in the network of flow channels. Moreover, the density of such mixture is assumed to be constant. The relationship between the viscosity of fluid mixture and hydrocarbon gas concentration can be described by using the following correlation (Turta et al., 1999):

$$\mu = \mu_o(a\cdot c + 1) \tag{10}$$

where μ_o denotes initial oil viscosity, mPa·s, which equals to 1.21 mPa·s in this study; $a = -1.603$; and c is concentration of hydrocarbon gas in vol% ($0 \le c < 58\%$). The mathematical model is solved by using commercial software (COMSOL version 4.2a), which is a package for the simulation of multiphysics or engineering application with the finite element method.

3. Packed-bed beads model

Sandstones are end products of a series of complex geological and hydrodynamic processes, i.e., sand grains from the quartz-bearing rocks that undergo transport, sedimentation, compaction and different forms of diagenesis (Bakke and Øren, 1997). In this study, a porous medium is simplified into a packed-bed beads model in two-dimensional (2D) space, assuming that grain size follows normal distribution (see Fig.

1). Such a simplified model is normally utilized as an effective substitute for porous media in the laboratory to identify the fluid flow mechanism (Dullien, 1992).

Various grain size distributions have been applied to effectively describe the real sandstone, e.g., log normal, binary and Weibull distribution (Gladkikh et al., 2008). It was found that the grain size distribution of Berea sandstone essentially follows normal distribution (Maloney et al., 1990). The radius of grain size (r) can then be obtained by using the following equation:

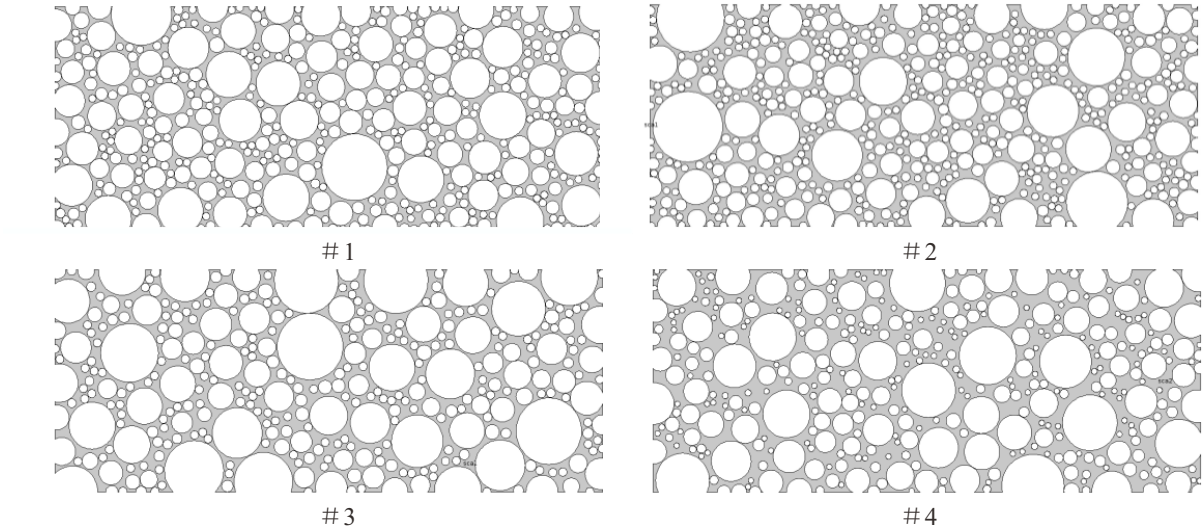

Fig. 1. Schematic of 2D packed-bed beads models for four scenarios (Note: The particle size distribution and pore throat distribution of the four models are shown in Figs. 2 and 3, respectively. Table 1 indicates the attributes of the four models).

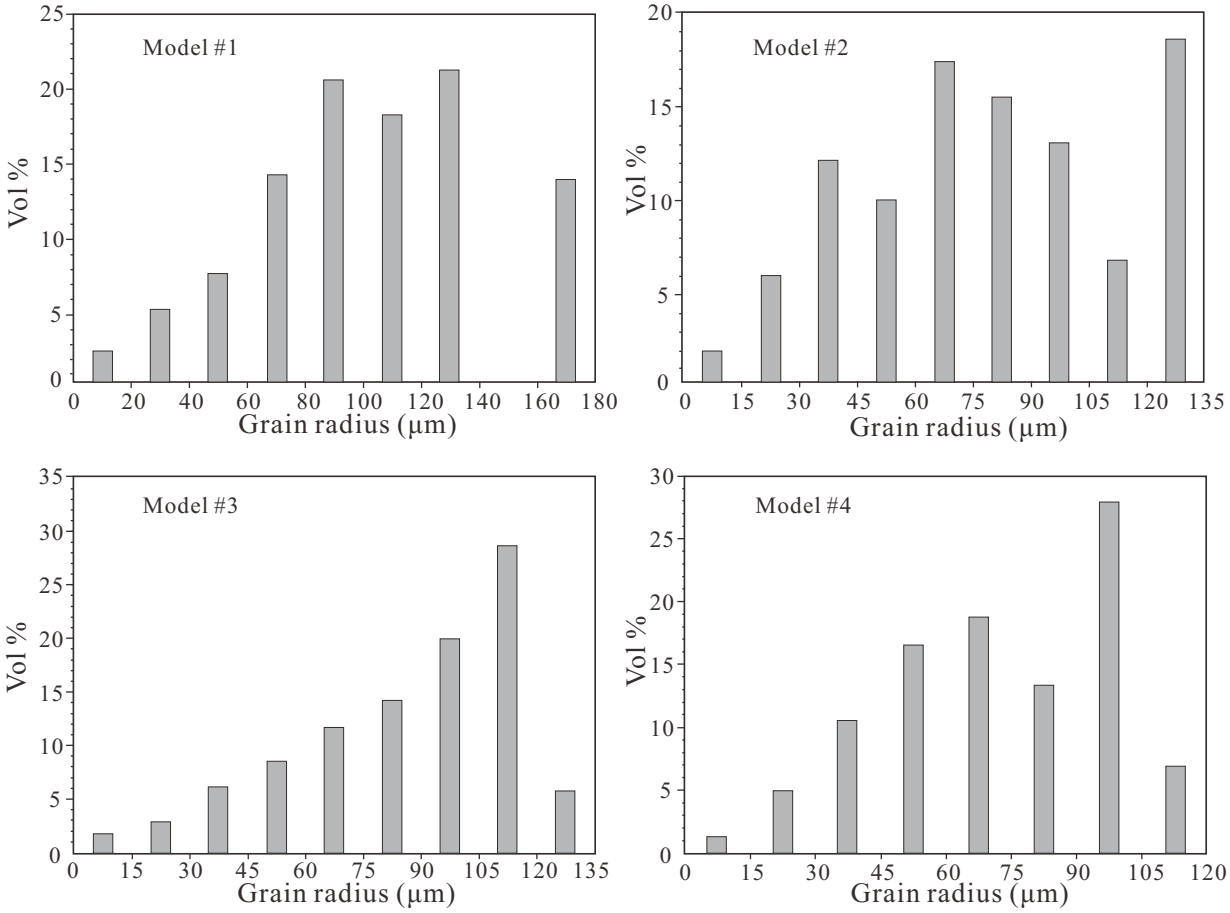

Fig. 2. Grain size distributions for four scenarios.

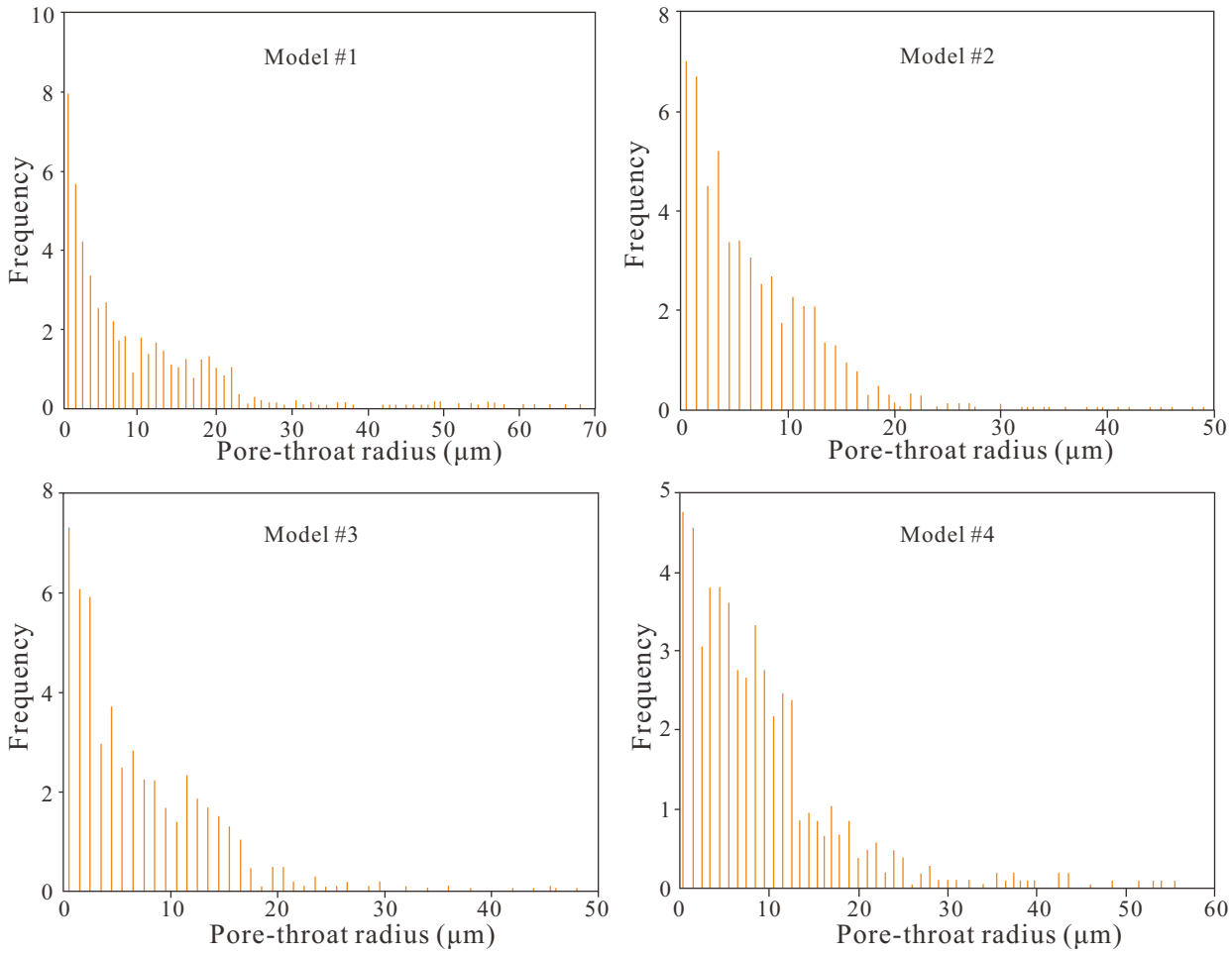

Fig. 3. Pore throat size distributions for four scenarios.

$$r = u \pm \sigma \sqrt{-2\ln\left(x_r \sigma \sqrt{2\pi}\right)} \tag{11}$$

where x_r is a normal random number between 0 and 1; and the mean and variance of normal distribution are u and σ^2, respectively. Figs. 2 and 3. show the grain size distributions and pore throat size distributions of the four packed-bed beads models, respectively. The model is mainly based on the sandstone characteristics of PI formation in the Daqing placanticline oilfield. The surface porosity is defined as the ratio of the void area in a plane cross-section of the porous medium to the total area of the cross-section (Dmitriev, 1995). In general, surface porosity can be considered to be the same as the porosity of porous media, provided that the pore structure is randomly distributed (Dullien, 1992). Hence, the porosity of the newly developed 2D model can be approximated through the surface porosity.

According to the Darcy's law:

$$v = -\frac{k}{\mu_l}\frac{\Delta P}{L} \tag{12}$$

where v denotes fluid velocity, m/s; k denotes permeability, mD; μ_l denotes fluid viscosity, Pa·s; L denotes the length of porous media, m; and ΔP is pressure drop between inlet and outlet of the porous medium, Pa. Once the pressure gradient and average fluid velocity are given, the permeability of the network of flow channels can be obtained. The heterogeneities of the grain size and pore throat size are quantified by using the Trask sorting coefficient (S_0), which can be calculated by using the following correlation (Fassnacht et al., 2003):

$$S_0 = \sqrt{\frac{d_{75}}{d_{25}}} \tag{13}$$

where d_{75} and d_{25} are the sizes (radii) of grains or pores that correspond to the 75th and the 25th percentile of their cumulative distribution.

4. Results and discussion

4.1 Effect of viscosity of fluid mixture

Physically, the viscosity of fluid mixture changes with the solvent concentration. Four porous media models are firstly constructed to examine the effect of viscosity on the concentration distribution. The different mean diameters and amounts of grain are assigned to each model to generate different distributions for permeability, porosity and pore throat size. The properties of these models are listed in Table 1. Figs. 2 and 3 respectively show the grain size distributions and pore throat size distributions for four scenarios. Fig. 4(a)

Table 1. Properties of porous media and the power-law coefficients between D_L/D_O versus Peclet number.

Model No.	Porosity (%)	Permeability (mD)	Trask sorting coefficient		Power-law coefficient
			Pore throat	Grain	
1	24.1	443	2.60	1.29	1.0482
2	28.9	630	2.24	1.42	1.0529
3	25.1	315	2.28	1.26	1.0505
4	35.2	2022	1.92	1.35	1.0706

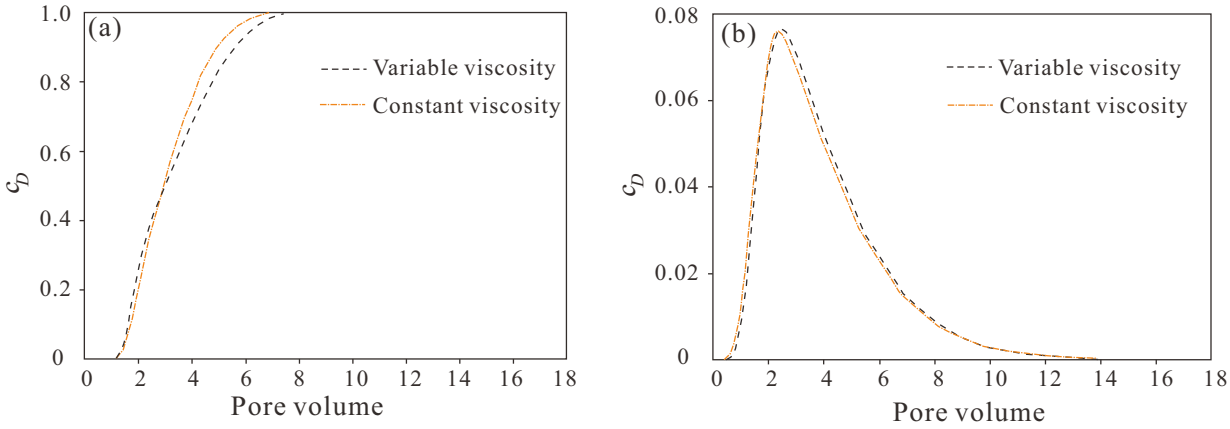

Fig. 4. Effluent concentration curves under (a) continuous solvent injection and (b) slug injection for Model #1 (Note: The injected pore volume of the two-dimensional model is calculated according to the area proportion of the model swept by the injected fluid).

presents the results of two scenarios with and without the variable viscosity of fluid mixture in Model #1. The width and length of the model is 4 and 7.5 mm, respectively. The variable viscosity of fluids mixture is found to result in a greater asymmetry of the concentration curve at the outlet than their constant viscosity, which is due to the viscosity decreasing with an increase in solvent concentration. Such variation of the mixture viscosity further results in a more seriously heterogeneous distribution of velocity field in the flow channels. At the pore scale, the velocity variation, which is caused by variable pore size, the bending of streamlines around the grains, and different velocity profiles within a pore, actually generates a dispersive flux (Ghazanfari et al., 2010). It is evident that the heterogeneity of velocity field resulting from the variable viscosity should have a similar effect on the dispersive flux, i.e., dispersion processes. Therefore, the heterogeneity of porous media is always considered as the major factor associated with the asymmetry of the concentration curve (Bijeljic et al., 2013), though the simulation results show that the variable viscosity of fluids mixture can also account for the "non-Fickian" transport phenomenon.

Solvent slug size is a significant optimization parameter for miscible flooding. In this study, based on the literature (Derakhshanfar et al., 2012; Song and Yang, 2012), 0.250 PV is used as representative slug size for miscible gas flooding. Variable viscosity leads to the situation that the range of concentration curve is larger than that for constant viscosity, although the shapes of their corresponding concentration curves are similar (see Fig. 4(b)). This may be attributed to the fact that the velocity difference among adjacent locations becomes greater due to variable viscosity.

4.2 Effect of heterogeneity on dispersion

Firstly, the performance of continuous hydrocarbon gas injection is numerically evaluated with a different Peclet number in the four models. Fig. 5(a) depicts the concentration curves of four scenarios with different Peclet numbers for Model #1. It can be seen that a longer tail of concentration curves is associated with a higher Peclet number. Compared to diffusion, with the increase in the Peclet number, advection gradually dominates the processes of solvent transport. It has been found in the previous section that the factors affecting the variation of velocity are determined by the heterogeneity of porous media and the properties of mixture. Therefore, when the Peclet number is increased, the heterogeneity of porous media imposes a larger impact on the concentration curves for a given fluid system, resulting in a more asymmetrical curve shape.

The non-flowing pores associated with heterogeneity are one of the main reasons for the non-Fickian or anomalous dispersion in porous media (Berkowitz et al., 2006). Fig. 5(b) shows the distribution of flow velocity in Model #1. As can be seen, there are only few main flow channels in the porous media, and the flow velocity in other parts is much smaller

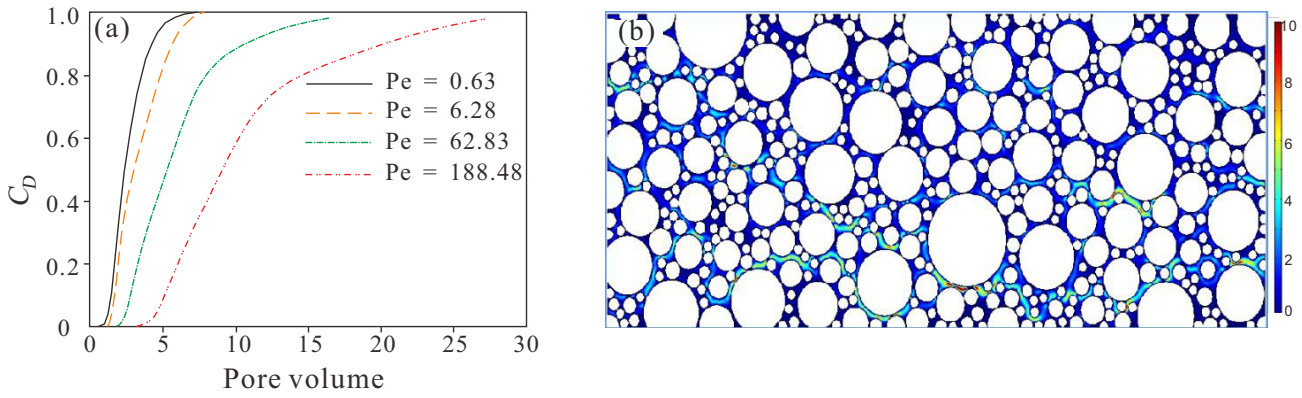

Fig. 5. (a) Dimensionless concentration curves with varying Peclet number at the outlet and (b) Dimensionless flow velocity distribution for Model #1.

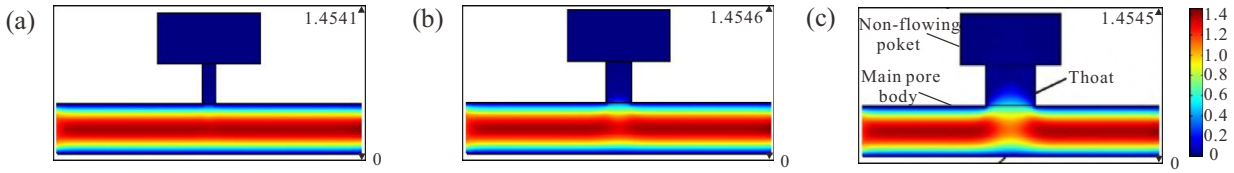

Fig. 6. Dimensionless velocity distribution with different aspect ratios for (a) 8, (b) 4, and (c) 2 at $c_D = 1.00$.

than that of the main flow channels, and is even close to zero.

In order to examine the effect of non-flowing pores on the flow performance of fluid mixture, a single non-flowing pore model is employed. The model consists of three parts, i.e., main pore body, non-flowing pocket and throat, with the latter connecting the other two. Fig. 6 shows the geometry of single non-flowing pore models with three aspect ratios. In this study, this is defined by the ratio of the horizontal length of non-flowing pocket to the horizontal length of throat, and velocity distribution. The main pore body diameter of the three models is 10 μm , and the non-flowing pocket width of the three models is 30 μm. The throat channel diameters of models (a), (b) and (c) are 3.75, 7.50 and 15.00 μm, respectively. The dimensionless average velocities of main pore body, non-flowing pocket and throat are in the range of 0.92–0.93, $5.24 \times 10^{-7} - 5.37 \times 10^{-3}$, and 0.01–1.11, respectively. This means that the primary flowing domain mainly includes the main pore body and the throat in the single non-flowing pore model. In this study, a flowing domain is defined as the average interstitial velocity of such domain that is higher than 0.1% of the total average flow velocity; conversely, it is called a non-flowing domain. It is found that the flowing domain of the throat part increases with an increase in throat size, while the liquid in the non-flowing pocket remains almost static. Obviously, the fluid in the non-flow pocket is also related to the length of the throat. To eliminate the influence of throat length, it is set the same for the three models.

Fig. 7 depicts the concentration curves of three models with different ratios of pore throat size but the same Peclet number. Logistic distribution is always utilized to match the concentration response (Scholze et al., 2001), and the results of simulation are fitted into the following model:

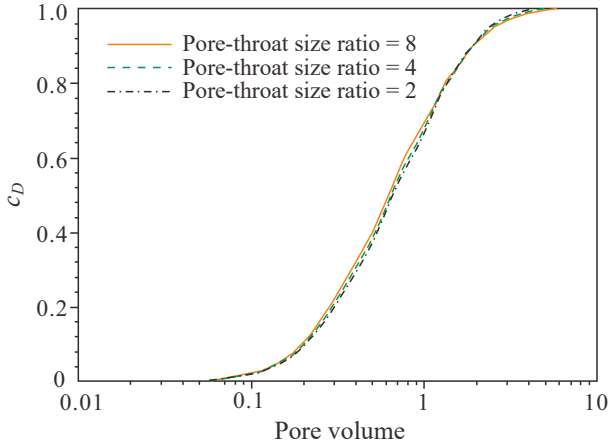

Fig. 7. Concentration curves of single non-flowing pore models.

$$c = \frac{\alpha}{1 + \left(\frac{V_{inj}}{\beta}\right)^{\gamma}} \tag{14}$$

where V_{inj} denotes the volume of injected fluid, ml; and α, β and γ are coefficients of the logistic distribution. There are monotonic correlations between the aspect ratios to coefficient γ and the aspect ratios to coefficient β (see Fig. 8).

Although there is only a minor difference among the concentration curves for the three models, a larger aspect ratio results in a higher solvent concentration and greater asymmetry of the concentration curve. More importantly, the dispersion coefficients of the three models gradually increase with an increase of the non-flowing domain (i.e., the ratio of non-flowing pore area to total area of the model, see Table 2). In this study, it is assumed that transverse dispersion is signifi-

Table 2. Properties of porous media and the power-law coefficients between D_L/D_O versus Peclet number.

Model		Percentage of non-flowing domain (%)	Dispersion coefficient ($\times 10^{-9}$ m^2/s)	Dimensionless average velocity
Single non-flowing pore model	Pore throat size ratio = 2	9.69	2.0534	0.7132
	Pore throat size ratio = 4	22.69	2.1903	0.8673
	Pore throat size ratio = 8	24.87	2.2908	0.9133
Packed-bed beads model	#1	10.46	2.8953	1.1125
	#2	5.43	2.6682	1.0562
	#3	6.67	2.7881	1.0697
	#4	4.61	2.4609	1.0472

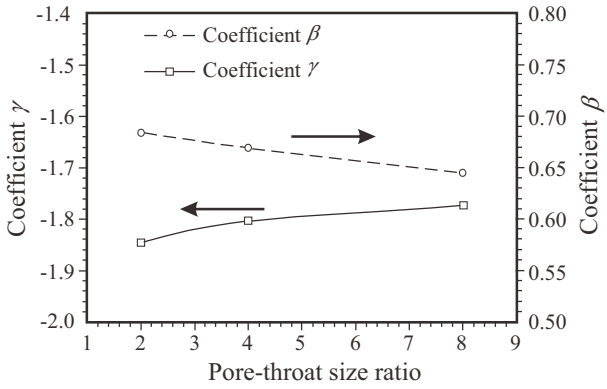

Fig. 8. Relationship between pore throat size ratio and coefficient γ of logistic distribution.

cantly smaller than longitudinal dispersion and that concentration can instantly reach equilibrium across the cross-section. Therefore, the dispersion coefficients of the four packed-bed beads models can be calculated with the one-dimensional analytical solution of the advection diffusion equation based on the simulation results. These dispersion coefficients are also found to increase as the non-flowing domain is increased (see Table 2), which is in good agreement with those of the single non-flowing pore model.

As for the single non-flowing pore model, a higher aspect ratio means a larger non-flowing domain, which objectively increases the heterogeneity of the model due to a greater difference between the pore size and the throat. For both types of model (i.e., single non-flowing pore model and packed-bed beads model), Table 2 presents an increase in the non-flowing domain, which implies a higher dimensionless interstitial velocity in the flowing domain at a fixed injection rate. It is evident that a higher velocity represents a stronger advective spreading effect on the transportation of solvent. Physically, the diffusion coefficient is a constant for a given system under equilibrium conditions, mainly depending on the properties of mixture, temperature and pressure (Duncan et al., 2005). As such, the diffusion coefficients are similar in all models. Strong advection and hydrodynamic dispersion will improve the dispersion processes of a solvent, resulting in a larger dispersion coefficient.

As listed in Table 1, the power-law coefficients of the four packed-bed beads models are found to be in the range of 1.04-1.08, which are in good agreement with those documented in the literature (Bijeljic et al., 2004). The Peclet numbers of the four models are identical, which implies that the diffusion process has the same effect on the solvent transport in these models because of the same coefficient (reciprocal of Peclet number) of the diffusion term in the dimensionless advection diffusion equation, i.e., Eq. (8). Meanwhile, the identical average interstitial velocities of the four models represent similar coefficients of the advection term of Eq. (8). Thus, once the boundary conditions and the initial conditions of Eq. (8) are the same, the difference of the concentration curves and the power-law coefficients shall result from the difference of interstitial velocity field of each model. In general, such variation of velocity is determined by the heterogeneity of porous media and fluid properties.

According to Table 1, there is no correlation between the power-law coefficients and Trask sorting coefficients of grain size. However, porosity, permeability and the Trask sorting coefficient of the pore throat size impose effects on the power-law coefficients. Higher permeability and porosity basically lead to a larger power-law coefficient, which is consistent with that of homogeneous porous media (Garmeh et al., 2009). It is worthwhile to note that there is a negative correlation between the Trask sorting coefficients of pore throat size and the power-law coefficients of these four models (see Table 1). This may be attributed to the fact that porosity, permeability and the Trask sorting coefficient can more effectively reflect the heterogeneity of various flow channels in porous media than the Trask sorting coefficient of grain size, which aims to describe the heterogeneity of a rock matrix. Especially, the Trask sorting coefficient of pore throat size directly represents the heterogeneity of flow channels, imposing a great influence on the interior flowing velocity of porous media.

As for solvent slug injection, simulations of four slug sizes are conducted for Model #1. Fig. 9(a) plots the concentration curves at the outlet for four scenarios with different slug sizes (0.125, 0.250, 0.375 and 0.500 PV). As can be seen,

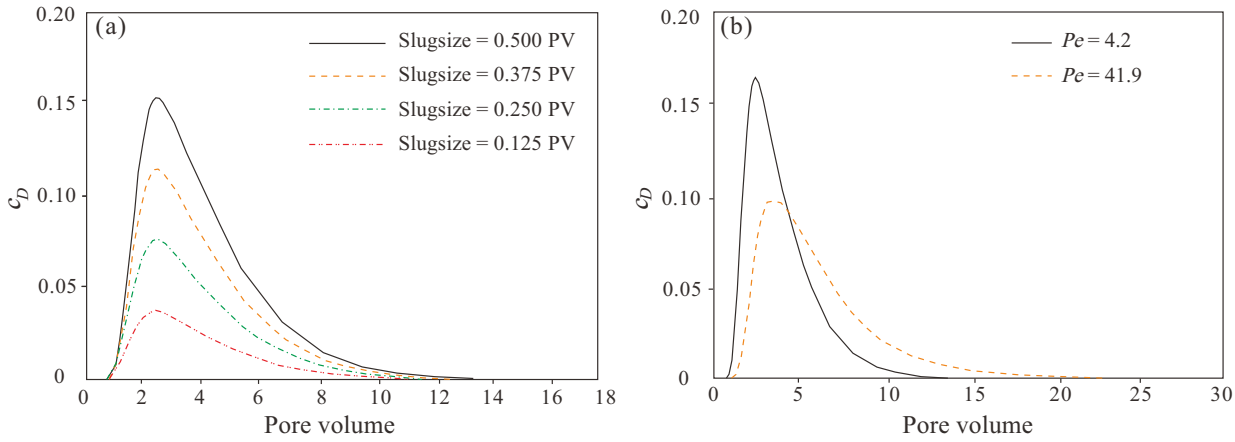

Fig. 9. Concentration curves at the outlet with (a) different slug sizes and (b) different Peclet numbers (slug size = 0.500 PV) for Model #1).

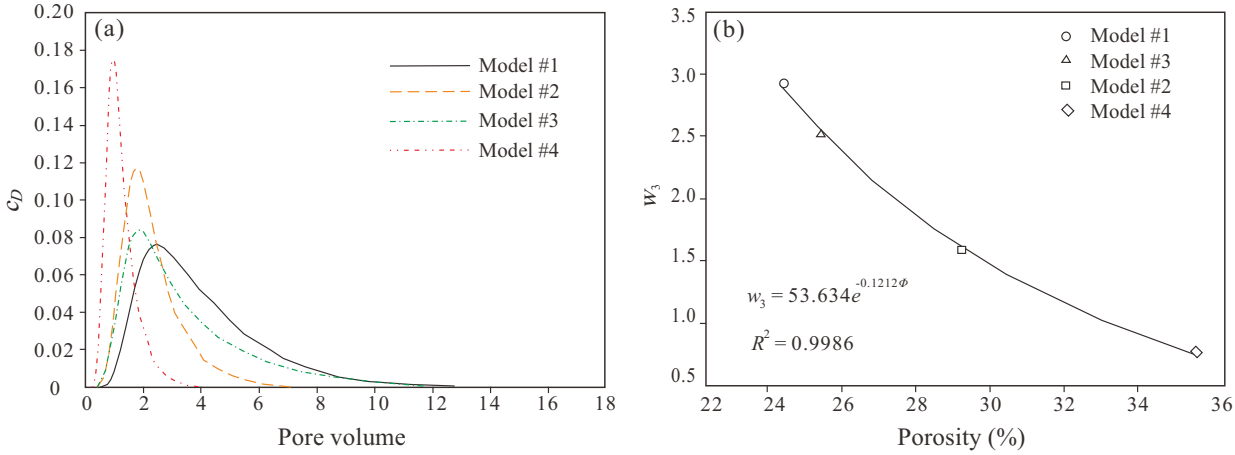

Fig. 10. (a) Concentration curves with 0.25 PV slug (*Pe* = 4.2); (b) Porosity versus coefficient w_3 of Weibull distribution for the four packed-bed beads models.

the concentration curves are not suitable to be matched with normal distribution due to the serious asymmetry. It is found that the four concentration curves almost reach their maximum values approximately at the same time. This is because when advection dominates the solvent transport, the dimension and distribution of mixing zone is determined by the velocity field of porous media. Thus, there are similar distributions of solvent slugs for the four scenarios due to a similar velocity distribution caused by the same porous media structure. A larger solvent slug size gives rise to higher maximum concentration due to more solvent. In addition, the injected fluid volumes at the inlet are almost the same for the four scenarios during the period of solvent slug completely passing through the outlet of the model. For example, when 95% of solvent flows out from the outlet of the porous media, the volumes of the injected fluids for the four scenarios are calculated to be 8.200, 8.000, 8.200, and 8.300 PV, respectively. This also implies that a larger slug size leads to a higher concentration of solvent rather than a longer longitudinal mixing zone (i.e., interior slug size of solvent) in porous media. This may be ascribed to the fact that the slug size of solvent is only associated with the amount of solvent, while it almost has no effect on the dispersion coefficients and velocity field of porous media.

Fig. 9(b) depicts the outlet fluid concentration with different Peclet numbers for Model #1. When the Peclet number is larger than 10, advection begins to contribute much more profoundly to solvent transport (Bijeljic et al., 2004). Thus, in this study, the Peclet numbers 4.2 and 41.9 are chosen as the representative samples for evaluating the effect of advection on solvent transport. A larger concentration but shorter mixing zone in porous media exists when the Peclet number is 4.2, as compared with the Peclet number of 41.9. Strong advection is found to stretch the slug size of solvent while the concentration of the mixture decreases. When 95% solvent flows out from the outlet for the scenarios of *Pe* = 4.2 and *Pe* = 41.9, the respective volumes of the injected fluids are found to be 8.400 and 17.600 PV, respectively. Obviously, stronger advection improves the mixing of solvent and increases the dispersion coefficient. As such, the dispersion coefficient for *Pe* = 41.9 is 11.5 times larger than that for *Pe* = 4.2.

The concentration curves of the four packed-bed beads

models with the same slug size and Peclet number were calculated and plotted in Fig. 10(a). As shown in the figure, larger porosity and permeability may lead to the earlier breakthrough of injected fluid and higher concentration at the production end. For the heterogeneous model, the lower the porosity and permeability, the smoother the concentration distribution at the production end.

The regressed curves are then applied to match the concentration curves. Furthermore, after analyzing the physical meaning of parameters in the regression model, the relationship between the geometrical features (phenomena) of concentration curves and the parameters of porous media and fluids (intrinsic properties) are explored. To achieve better curve fitting results, logistic distribution, Gauss distribution and Weibull distribution are employed to match the concentration curves. The average R^2 coefficient of four packed-bed beads models with these three regression functions are found to be 0.866, 0.891 and 0.992, respectively. The Weibull distribution $(f(t))$ can be used to more accurately represent the geometrical features compared to other regression models. The corresponding function with four parameters is provided as follows:

$$f(t)=\begin{cases}0 & \\ v\le v_0-w_3\left(\dfrac{w_2-1}{w_2}\right)^{\frac{1}{w_2}} & \\ w_1\left(\dfrac{w_2-1}{w_2}\right)^{\frac{w_2-1}{w_2}}\left[\left(\dfrac{v-v_0}{w_3}\right)+\left(\dfrac{w_2-1}{w_2}\right)^{\frac{1}{w_2}}\right]^{w_2-1}-\left\{\left[\dfrac{v-v_0}{w_3}+\left(\dfrac{w_2-1}{w_2}\right)^{\frac{1}{w_2}}\right]^{w_2}+\dfrac{w_2-1}{w_2}\right\} & \\ v>v_0-w_3\left(\dfrac{w_2-1}{w_2}\right)^{\frac{1}{w_2}} & \end{cases} \tag{15}$$

Table 3. Parameters of Weibull distribution for matching the concentration curves.

Model No.	w_1	w_2	w_3	v_0	R^2
#1	0.1646	1.4939	2.7978	2.543	0.9916
#2	0.3288	1.8789	1.5630	1.9463	0.9907
#3	0.1738	1.3084	2.5061	1.8765	0.9927
#4	0.3636	1.7049	0.9320	1.2092	0.9891

The regressed four parameters (w_1, w_2, w_3, and v_0) together with the corresponding R^2 are tabulated in Table 3. Here, w_1 mainly controls the maximum of distribution; w_2 (shape parameter) has an effect on the shape of Weibull distribution; w_3 (scale parameter) affects the scale of distribution along the abscissa; v_0 (location parameter) can provide the position information about distribution on the x axis. It is found that the maximum concentration is mainly affected by porosity, permeability, and the area of non-flowing pores. In particular, porosity and parameter w_3 (i.e., scale parameter) shows an exponent correlation. As shown in Fig. 10(b), a larger porosity value may lead to a broader solvent slug distribution.

5. Conclusions

In this work, a mathematical model has been developed to quantitatively examine the effect of the properties of both porous media and fluids on dispersion at the pore scale during miscible flooding processes. Consequently, the solvent transport process is numerically described with 2D porous media models. It is found that the variable viscosity of fluid mixture is one of the factors accounting for non-Fickian transport because of the strong heterogeneity of velocity field caused by variable viscosity. The calculated dispersion coefficients show that a larger ratio of non-flowing domain can result in a higher dispersion coefficient. This is possibly because a larger ratio of non-flowing domain leads to a higher interstitial velocity and stronger advective spreading. Meanwhile, a negative correlation is found between the power-law coefficients and Trask sorting coefficients of pore throat size. This negative correlation is likely because the latter is a parameter that reflects the heterogeneity of flow network. Such heterogeneity always has a great impact on the dispersion processes. As for slug injection, a larger slug size leads to a higher solvent slug concentration, but not to a longer longitudinal dimension of mixing, because the dispersion coefficient and velocity field are not affected by slug size. Both a larger Peclet number and a larger porosity value result in a broader solvent slug, that is, a longer mixing zone in porous media.

Acknowledgement

The research was supported by the Key Fund Project of the National Natural Science Foundation of P. R. China (Grant No. 51834005).

Conflict of interest

The authors declare no competing interest.

References

Arshad, A., Al-Majed, A. A., Maneouar, H., et al. Carbon dioxide (CO_2) miscible flooding in tight oil reservoirs: A case study. Paper SPE 127616 Presented at SPE Kuwait International Petroleum Conference and Exhibition, Kuwait City, Kuwait, 14-16 December, 2009.

Babaei, M., Joekar-Niasar, V. A transport phase diagram for pore-level correlated porous media. Advances in Water

Resources, 2016, 92: 23-29.

Bakke, S., Øren, P.-E. 3-D pore-scale modeling of sandstones and flow simulations in the pore networks. SPE Journal, 1997, 2(2): 136-149.

Berkowitz, B., Cortis, A., Dentz, M., et al. Modeling non-Fickian transport in geological formations as a continuous time random walk. Reviews of Geophysics, 2006, 44(2): 2005RG000178.

Berkowitz, B., Scher, H. The role of probabilistic approaches to transport theory in heterogeneous media. Transport in Porous Media, 2001, 42(1): 241-263.

Bijeljic, B., Mostaghimi, P., Blunt, M. J. Insights into non-fickian solute transport in carbonates. Water resources research, 2013, 49(5): 2714-2728.

Bijeljic, B., Muggeridge, A. H., Blunt, M. J. Pore-scale modeling of longitudinal dispersion. Water resources research, 2004, 40(11): W11501.

Booth, R. Miscible flow through porous media. Oxford, University of Oxford, 2008.

Bretz, R. E., Orr, Jr. F. M. Interpretation of miscible displacements in laboratory cores. SPE Reservoir Engineering, 1987, 2(4): 492-500.

Bretz, R. E., Specter, R. M., Orr, Jr. Mixing during single phase flow in reservoir rocks: Models, effects of pore structure and interpretation of experiments, in Reservoir Characterization, edited by L. W. Lake and H. B. Carrol, Jr., Dallas, Texas, pp. 585-642, 1986.

Bretz, R. E., Specter, R. M., Orr Jr., F. M. Effect of pore structure on miscible displacement in laboratory cores. SPE Reservoir Engineering, 1988, 3(3): 857-866.

Brodie, J. A., Jhaveri, B. S., Moulds, T. P., et al. Review of gas injection projects in BP. Paper SPE 154008 Presented at SPE Improved Oil Recovery Symposium, Tulsa, Oklahoma, 14-18 April, 2012.

Cao, J., Kitanidis, P. K. Pore-scale dilution of conservative solutes: An example. Water Resources Research, 1998, 34(8): 1941-1949.

Correa, A. C., Pande, K. K., Ramey, H. J., et al. Computation and interpretation of miscible displacement performance in heterogeneous porous media. SPE Reservoir Engineering, 1990, 5(1): 69-78.

Delgado, J. M. P. Q. Longitudinal and transverse dispersion in porous media. Chemical Engineering Research and Design, 2007, 85(9): 1245-1252.

Derakhshanfar, M., Nasehi, M., Asghari, K. Simulation study of CO_2-assisted waterflooding for enhanced heavy oil recovery and geological storage. Paper CMTC-151183-MS Presented at Carbon Management Technology Conference, Orlando, Florida, 7-9 February, 2012.

Dmitriev, N. M. Surface porosity and permeability of porous media with a periodic microstructure. Fluid Dynamics, 1995, 30(1): 64-69.

Dullien, F. A. L. Porous Media, Fluid Transport and Pore Structure. New York, USA, Academic Press, 1992.

Duncan, B., Urquhart, J., Roberts, S. Review of measurement and modelling of permeation and diffusion in polymers. Teddington, UK, National Physical Laboratory Report, 2005.

Fassnacht, H., McClure, E. M., Grant, G. E., et al. Downstream effects of the pelton-round butte hydroelectric project on bedload transport, channel morphology, and channel-bed texture, lower deschutes river, Oregon. Oregon Water Science and Application, 2003, 7: 175-207.

Fourar, M., Konan, G., Fichen, C., et al. Tracer tests for various carbonate cores using X-ray CT. Paper SCA200556 Presented at Annual International Symposium of the Society of Core Analysis, Toronto, Canada, 21-25 August, 2005.

Garmeh, G., Johns, R. T., Lake, L. W. Pore-scale simulation of dispersion in porous media. SPE Journal, 2009, 14(4): 559-567.

Ghazanfari, M. H., Kharrat, R., Rashtchian, D., et al. Statistical model for dispersion in a 2D glass micromodel. SPE Journal, 2010, 15(2): 301-312.

Gladkikh, M., Chen, J., Chen, S. Method of determining formation grain size distribution from acoustic velocities and NMR relaxation time spectrum. Paper SPWLA-2008-GGG Presented at SPWLA 49th Annual Logging Symposium, Austin, Texas, 25-28 May, 2008.

Golparvar, A., Zhou, Y., Wu, K., et al. A comprehensive review of pore scale modeling methodologies for multiphase flow in porous media. Advances in Geo-Energy Research, 2018, 2(4): 418-440.

Jha, R. K., John, A., Bryant, S. L., et al. Flow reversal and mixing. SPE Journal, 2009, 14(1): 41-49.

Mahnaz, H., Mitra, D., Muhammad, S. Pore-network simulation of unstable miscible displacements in porous media. Transport in Porous Media, 2016, 113(3): 511-529.

Maloney, D. R., Honarpour, M. M., Brinkmeyer, A. D. The effects of rock characteristics on relative permeability. Office of Scientific and Technical Information, United States, 1990.

Majdalani, S., Chazarin, J. P., Delenne, C., et al. Solute transport in periodical heterogeneous porous media: Importance of observation scale and experimental sampling. Journal of Hydrology, 2015, 520: 52-60.

Muhammad, K. A., Athari, A. O., Abubakar, J. A., et al. Influence of permeability and injection orientation variations on dispersion coefficient during enhanced gas recovery by CO_2 injection. Energies, 2019, 12(12): 2328.

Panja, P., Velasco, R., Deo, M. Understanding and modeling of gas-condensate flow in porous media. Advances in Geo-Energy Research, 2020, 4(2): 173-186.

Peyman, M., Saeed, T., Steven, L. B., et al. Solvent diffusion and dispersion in partially saturated porous media: An experimental and numerical pore-level study. Chemical Engineering Science, 2018, 191: 300-317.

Sahimi, M., Rasaei, M. R., Haghighi, M. Gas injection and fingering in porous media, in Theory and Applications of Transport in Porous Media, edited by S. M. Hassanizadeh, Springer, Dordrecht, pp. 133-168, 2006.

Saied, A., Hejazi, S. H., Apostolos, K. Longitudinal dispersion in heterogeneous layered porous media during stable and unstable pore-scale miscible displacements. Advances in Water Resources, 2018, 119: 125-141.

Scholze, M., Boedeker, W., Faust, M., et al. A general best-

fit method for concentration-response curves and the estimation of low-effect concentrations. Environmental Toxicology and Chemistry, 2001, 20(2): 448-457.

Sheng, G., Su, Y., Zhao, H., et al. A unified apparent porosity/permeability model of organic porous media: Coupling complex pore structure and multi-migration mechanism. Advances in Geo-Energy Research, 2020, 4(2): 115-125.

Song, C., Yang, D. Optimization of CO_2 flooding schemes for unlocking resources from tight oil formations. Paper SPE 162549 Presented at SPE Canadian Unconventional Resources Conference, Calgary, Alberta, 30 October-1 November, 2012.

Srivastava, R. K., Huang, S. S., Dong, M. Laboratory investigation of Weyburn CO_2 miscible flooding. Journal of Canadian Petroleum Technology, 2000, 39(2): 41-51.

Turta, A., Fisher, D., Singhal, A. K., et al. Variation of oil-solvent mixture viscosity in relation to the onset of asphaltene flocculation and deposition. Journal of Canadian Petroleum Technology, 1999, 38(13): PETSOC-99-13-46.

Wen, Y., Kantzas, A. Evaluation of heavy oil/bitumen-solvent mixture viscosity models. Journal of Canadian Petroleum Technology, 2004, 45(4): 56-61.

Yang, X., Lu, W., Jin, X., et al. Fractal theory-based seepage model of hershel-bulkley fluid in porous medium. Coal Geology & Exploration, 2020, 48(3): 122-127. (in Chinese)

Yang, X., Scheibe, T. D., Richmond, M. C., et al. Direct numerical simulation of pore-scale flow in a bead pack: Comparison with magnetic resonance imaging observations. Advances in Water Resources, 2013, 54: 228-241.